Journal of Polymers and the Environment (2020) 28:1315–1325
https://doi.org/10.1007/s10924-020-01688-w

ORIGINAL PAPER

The Effect of Carbodiimide on the Stability of Wood Fiber/Poly(lactic acid) Composites During Soil Degradation

Ce Sun[1] · Zixiang Huang[1] · Yifan Liu[1] · Changxin Li[1] · Haiyan Tan[1] · Yanhua Zhang[1]

Published online: 2 March 2020

Abstract

To prolong the service lives of wood fiber (WF)/poly(lactic acid) (PLA) composites, composites with different contents of bis (2,6-diisopropylphenyl) carbodiimide (BDICDI) were prepared. The composites were buried in natural soil for 150 days to evaluate the stabilizing effect of BDICDI on the WF/PLA composites. It was also used to evaluate the properties changes of WF/PLA composites under extreme conditions. The changes in the chemical structures, molecular weights and thermal properties of the WF/PLA composites during soil burial and the stabilization mechanism of BDICDI on the composites were studied. The results showed that the addition of BDICDI reacted with both the formed acid and the water absorbed by the WF/PLA composites, which inhibited the breaking of ester bonds in the WF/PLA composites. After 120 days of soil burial, the tensile strengths of the WF/PLA/1 wt% BDICDI composites were 1.31 times to those of the WF/PLA composites. This research provided theoretical support to prolong the service lives of WF/PLA composites and expanded the application scope of WF/PLA composites.

Graphic Abstract

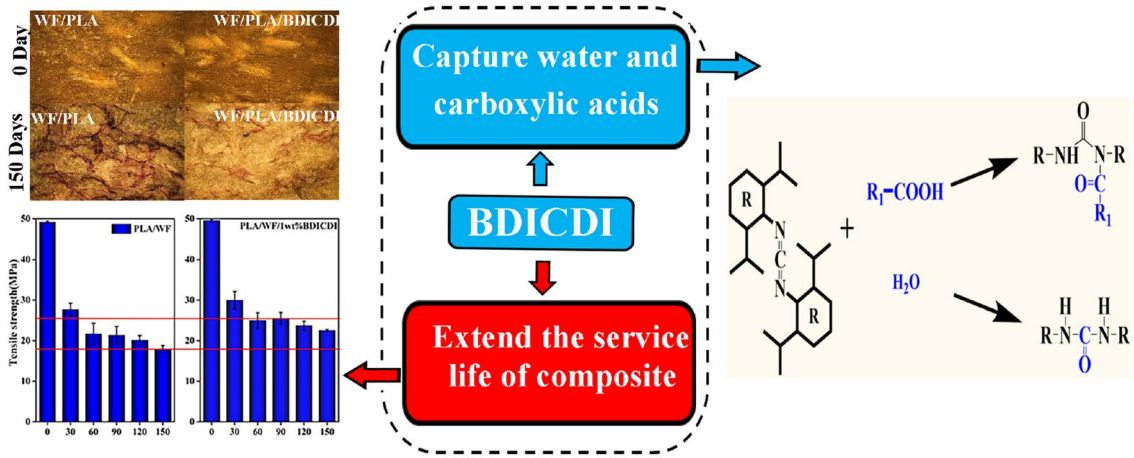

Keywords Poly(lactic acid) · Wood fiber · Carbodiimide · Soil burial degradation

Introduction

By 2016, the global production of petroleum-based plastics has reached 335 Million tons and half of these plastics litter continents and oceans after use [1, 2]. Petroleum-based plastics gradually break down into smaller fragments and are easily eaten by animals [3–5]. It is estimated that 99%

✉ Yanhua Zhang
zhangyanhua@nefu.edu.cn

[1] Key Laboratory of Bio-Based Material Science and Technology, Ministry of Education, Northeast Forestry University, Harbin 150040, China

of seabirds will regularly uptake discarded plastic by 2050 and that such behavior is destructive to birds [6, 7]. Recently, plastic residues have also been detected in human bodies and have induced negative effects on human bodies, such as gastrointestinal dysfunction, reproductive difficulties [8, 9]. The main source of plastic pollution is disposable plastics with short service lives, such as plastic bags, and agricultural films [10, 11]. In recent years, renewable bioplastics are expected to solve the problem of petroleum-based plastic pollution. PLA with good biodegradability is a kind of thermoplastic biopolyester derived from starch [12]. Although PLA shows similar properties to other petroleum-based plastics that widely used in packaging and agriculture fields, some properties still need to be improved [13]. Wood fiber (WF) is a kind of cheap and nontoxic renewable biomass resource. As the structural skeleton of WF/PLA composites, wood fiber improves the impact resistance and formability of PLA. Additionally, the cost of PLA can be further reduced after adding wood fiber [14, 15]. WF/PLA composites are completely degradable and have good promotion prospects. If eaten by organisms after being discarded, WF/PLA composites can be degraded and excreted from the bodies. WF/PLA composites still need to maintain a certain stability during use. For example, when WF/PLA composites are used as plant breeding pots or agricultural films, the composites need to maintain a certain mechanical property within a few months of plant growth. However, WF/PLA composites are very sensitive to the environment. Water from the environment penetrates into WF/PLA composites through the wood fibers, and converts PLA into small molecules [16]. Microorganisms from the environment then mineralize and assimilate these small molecules during use [17]. The strength or stiffness of WF/PLA composites decrease drastically when the humidity of the environment is too high [18, 19]. In addition, the presence of binding water in WF can hydrolyze the ester bonds of PLA during thermal processing, which promotes the fracture of the PLA molecular chains [20]. WF/PLA composites exhibit poor stability, which greatly limits the use and promotion of WF/PLA composites [26]. Therefore, it is necessary to find a stabilizer to maintain the stability of WF/PLA composites. The PLA stabilizers found in the current research are isocyanates, acid chlorides and acid anhydrides [21, 22]. These stabilizers can capture the bound water released by the WF during thermal processing, while stabilizing the ester bond in the PLA to inhibit degradation. Although the addition of these stabilizers improves the stability of the composites, the treated PLA is no longer completely degradable. Additionally, the stabilizer itself is harmful to the environment and cannot be applied to food packaging materials or agricultural materials. Bis (2,6-diisopropylphenyl) carbodiimide (BDICDI) is not classified as a hazardous material by the European Chemicals Agency [23]. Also, BDICDI is an effective acid and water removal agent, and thus BDICDI hinders the hydrolysis and thermal degradation of polyester plastics [24, 25]. It was confirmed that the addition of BDICDI effectively inhibited the degradation of WF/PLA composites during processing [26]. However, the mechanism by which BDICDI affects the stability of WF/PLA composites in a real environment has not been studied. At the same time, the property changes of WF/PLA and WF/PLA/BDICDI composites in real environment also needs to be investigated.

In this work, WF/PLA composites with different mass contents of BDICDI were buried in real soil condition for 150 days. The purpose of this work is to investigate the stable effect of BDICDI on WF/PLA composites in a real environment, and to explore the stabilization mechanism of BDICDI on WF/PLA/BDICDI composites. At the same time, soil burial can also be used to simulate the use of composites under extreme conditions, so as to provide some references for WF/PLA/BDICDI composites to replace disposable plastics with short service lives. Using tensile test, differential scanning calorimetry (DSC) and upright light microscope, the amount of BDICDI that is suitable for WF/PLA composites was explored, and the specific effect of BDICDI on the stability of the composites was evaluated. Also, the stabilization mechanism of BDICDI on WF/PLA composites was investigated by various means. This approach provides a theoretical basis for WF/PLA composites to replace nondegradable petroleum-based plastics and to expand the application of WF/PLA composites in daily life.

Experimental Section

Materials

PLA (Ingeo 4032D) with a density of 1.24 g cm^{-3}, containing 2% D-lactic acid was purchased from Nature Works (USA). Poplar wood fiber (WF) was supplied by Linyi Fengming wood flour factory (Shandong, China). The sizes of wood fiber are between 0.56 and 1.12 mm. Bis (2,6-diisopropylphenyl) carbodiimide (AW700) was purchased from Yin yuan New Materials Co., Ltd (Guangzhou, China).

Sample Preparation

The PLA pellets was dried in vacuum oven at 80 °C for 6 h, while wood fiber was dried at 120 °C for 10 h. These operations were designed to remove moisture as much as possible. Wood fiber, PLA pellets and BDICDI additive (Table 1) were extruded with a twin-screw extruder (SHJ-20, Nanjing Jeante Co., Ltd.). The ratio of the quality of various raw materials were shown in Table 1. The temperature in the extruder was 135–175–180–175–135 °C

Table 1 The ratio of the quality of various raw materials

Sample	PLA/wt%	WF/wt%	BDICDI/wt%
1	100	0	0
2	70	30	0
3	70	30	1
4	70	30	3

(from hopper to die). Finally, the bones like composite samples were obtained through injection molding with the following temperature in the injection molding: 170–175–180–170 °C (JPH180C, Guangdong ONLY Machinery Co., Ltd.).

All the samples were buried in the campus of Xinhua Printing Factory (Harbin, China), and the samples were buried at a depth of 10–15 cm. From 2018-Apr-28 to 2018-Sep-25, the average precipitation of each month is 25 mm, 65 mm, 55 mm, 80 mm, 160 mm, 45 mm (from Apr. to Sep.). And the average temperature of each month during soil burial is 5.8 °C, 12.8 °C, 20.1 °C, 22 °C, 20.3 °C, 14.1 °C(from Apr. to Sep.). Samples buried in the soil were removed every 30 days and washed with distilled water for three times. The samples were then dried in a blast oven at 35 °C for two weeks for subsequent testing.

Fourier Transform Infrared Spectroscopy (FTIR)

Fourier transform infrared spectroscopy (Tensor II, Bruker) using ATR was used to collect the spectra of samples with the range of 600–4000 cm^{-1}. The resolution is 4 cm^{-1} and all the data were performing analyzed by using OPUS 7.5 (Bruker).

X-ray Photoelectron Spectroscopy (XPS)

The element composition of samples with different burial intervals was investigated by XPS (XPS, K-Alpha, Thermo Fisher Scientific Co., Ltd). Monochromatic Al Kα radiation (1486.6 eV) was used to carry out the analysis.

Gel Permeation Chromatography/Light Scattering Instrument (GPC/LS) Analysis

The refractive index increment (dn/dc) for different burial intervals were obtained from GPC/LS coupled system with a Light Scattering Instrument (DAWN HELEOS II, American) and a Varian 9012Q pump. Tetrahydrofuran was used as mobile phase at a constant flow speed of 1 mL/min.

Mechanical Analysis

The tensile strength of the composites with different burial time were performed by CMT-5504 Universal Testing Machine (Shenzhen SANS Test Machine Co., Ltd. China). According to the ASTM D638-10, samples was tested at a crosshead speed of 5 mm/min. At least five samples were tested to get an averaged value.

Light Upright Microscope

Light upright microscope (Olympus, BX53M) was used to characterize the surface changes of WF/ PLA composites before and after soil burial. All images are integrated the microscope hardware setup with the Olympus Stream image analysis software.

Differential Scanning Calorimetry (DSC)

Thermal analysis of samples with a weight of 3–5 mg was performed using NETZSCH DSC 204 instrument. Samples were heated from 20 to 200 °C and kept for 5 min at 200 °C. Then, the samples were quenched to − 20 °C and finally heated back to 200 °C. All the heating rates were 10 °C/min. The crystallinity formula used was:

$$Xc = \frac{\Delta H_m - \Delta H_c}{\Delta H_m^0} \times \frac{100}{\omega} \quad (1)$$

where, ΔH_m^0 is 100% pure crystalline PLA with a melting enthalpy of 93.6 J/g. ΔH_m is the melting enthalpy, ΔH_c is the cold crystallization enthalpy, ω is ratio of PLA in WF/PLA composites.

Results and Discussion

Chemical Stability Mechanism

FTIR spectras (Fig. 1) were used to study the chemical structures by observing changes in the infrared peaks. During 150 days of soil burial, new peaks belonging to vibrations of amide I (1649 cm^{-1}) and amide II (1540 cm^{-1}) were gradually formed in two WF/PLA/BDICDI composites and the intensities of the peaks gradually increased. In the early stage of soil degradation, hydrolysis is the main cause of PLA degradation. In addition, the carboxyl acid formed by PLA chain cleavage catalyzes the degradation of PLA [27, 28]. During the degradation process of PLA, carboxylic acid was formed due to the hydrolysis of the ester bond. Carboxylic acid in turn promoted the degradation of the ester bonds and this phenomenon is called autocatalytic

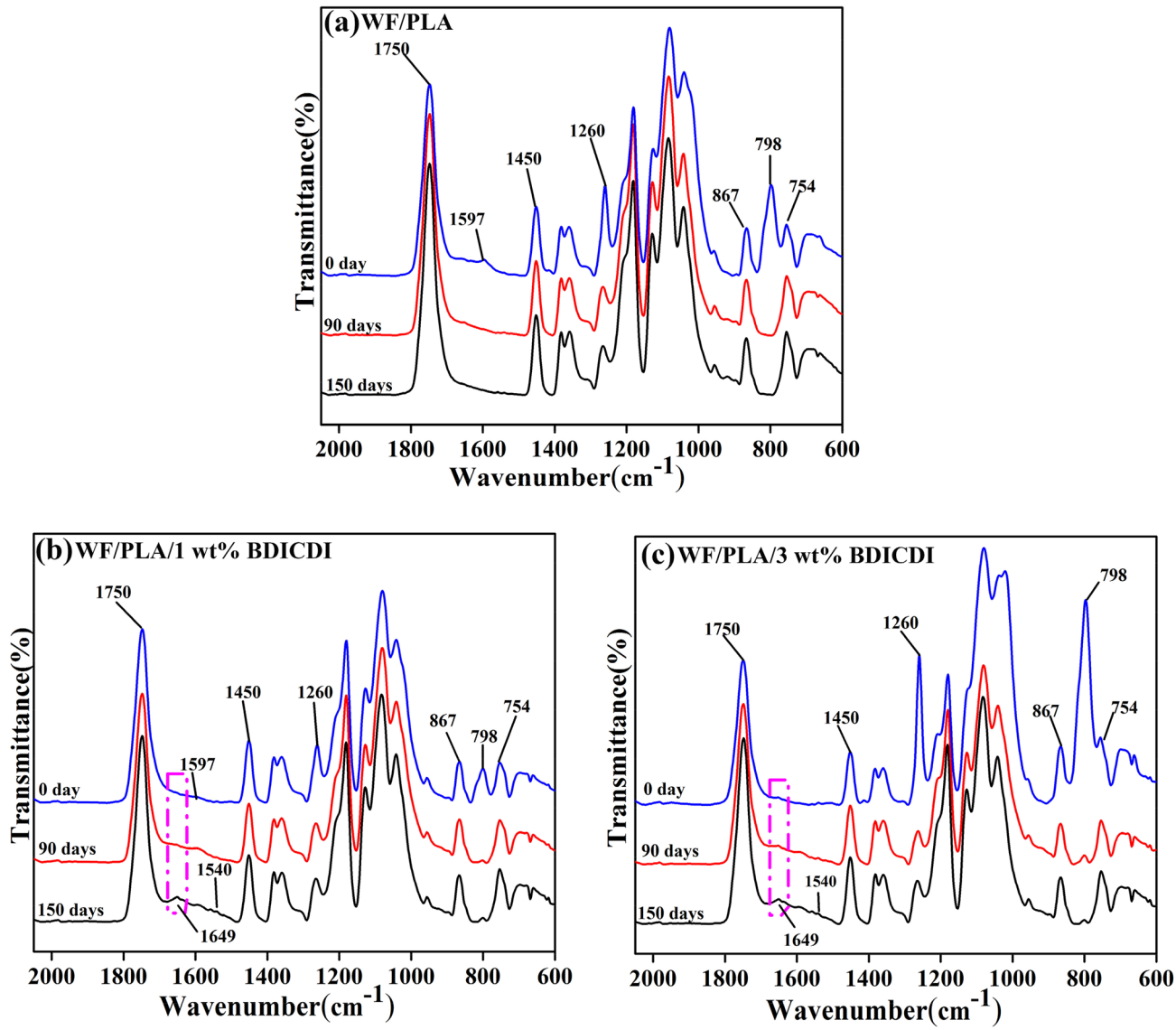

Fig. 1 The FTIR spectra of **a** WF/PLA, **b** WF/PLA/1 wt% BDICDI, **c** WF/PLA/3 wt% BDICDI composites before and after soil burial

degradation of PLA. BDICDI reacts with the water and carboxylic acid from the WF/PLA/BDICDI composites, and the imine bonds in BDICDI gradually convert to amide bonds (Fig. 4) [23, 29]. These two reactions inhibited the degradation of the composites. As the soil burial time increased, C=O stretching of the ester bond (1750 cm^{-1}) shifted toward lower wavenumbers. This finding demonstrated that after 150 days of soil burial, many ester groups in the PLA chains were destroyed [30].

In addition, the bending vibration of ester bonds at 1260 cm^{-1} was substantially shifted, and the amount of BDICDI was negatively correlated with the peak shift (Fig. 2) [31]. To explain this phenomenon, XPS analysis of the composites was performed to study the changes in the functional groups of WF/PLA composites (Fig. 3). The

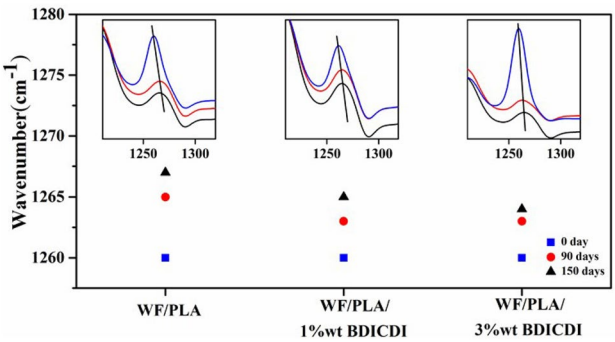

Fig. 2 Peak shift of three WF/PLA composites at 1260 cm^{-1}

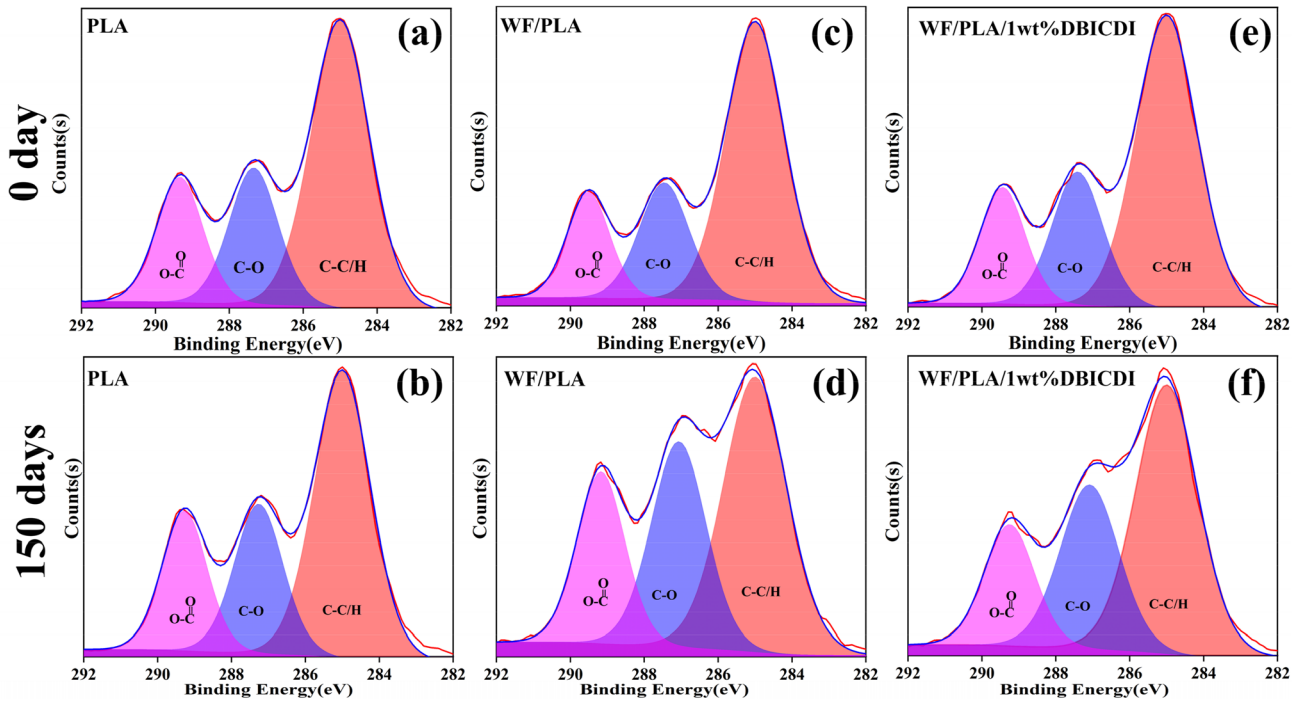

Fig. 3 XPS C1s spectra of **a** PLA, **c** WF/PLA, **e** WF/PLA/1 wt% BDICDI composites; XPS C1s spectra of **b** PLA, **d** WF/PLA, **f** WF/PLA/1 wt% BDICDI composites after soil burial of 150 days

Table 2 The percentage different chemical bonds in PLA

Time (day)	PeakBE (eV)	Chemical bond	Percentage (%)
0	285.00	C–C/H	57.45
	287.46	C–O	22.74
	289.51	O–C=O	19.82
150	285.00	C–C/H	54.27
	287.46	C–O	24.53
	289.51	O–C=O	21.21

Table 3 The percentage different chemical bonds in WF/PLA composite

Time (day)	PeakBE (eV)	Chemical bond	Percentage (%)
0	285.00	C–C/H	61.32
	287.46	C–O	21.76
	289.51	O–C=O	16.91
150	285.00	C–C/H	47.29
	287.46	C–O	30.48
	289.51	O–C=O	22.23

Table 4 The percentage different chemical bonds in WF/PLA/ 1 wt% BDICDI composites

Time (day)	PeakBE (eV)	Chemical bond	Percentage (%)
0	285.00	C–C/H	59.71
	287.46	C–O	22.65
	289.51	O–C=O	17.64
150	285.00	C–C/H	51.48
	287.46	C–O	29.71
	289.51	O–C=O	18.81

percentage of different chemical bonds in PLA or PLA composites were shown in Tables 2, 3, and 4. C1s peak shows the presence of three carbon groups in PLA, including C–C/H at 285.00 eV, C–O at 287.46 eV, and O=C–O at 289.51 eV in PLA [32, 33]. To better analyze the changes in functional groups of the WF/PLA composites, the changes of pure PLA before and after 150 days of soil burial were used as a reference. After 150 days of soil burial, the proportion of C–C/H bonds in pure PLA decreased from 57.45 to 54.27% while the proportions of C–O bonds and O–C=O bonds increased, and the increased degree of the C–O bonds and C = O bonds were similar (Table 3). This finding indicated that one ester bond was broken down under the action of water molecules during the degradation process. And a carboxyl group and a hydroxyl group were formed. It was demonstrated that the proportional increases in the C–O bonds and O–C=O bonds were similar. After 150 days of degradation, the reduction of C–C ratio in the WF/PLA composites was 4.37 times to

that in pure PLA. This difference was attributed to the presence of wood fiber, which acted as a transport medium for water, thereby promoting the degradation of the WF/PLA composites [26]. The rising ratios of the C–O and O–C=O bonds were still similar. The broken ester bonds led to a decrease in the proportion of C–C bonds and similar increases in the proportions of C–O and O–C=O bonds. For the WF/PLA/1 wt% BDICDI composites, the decreasing ratio of C–C/H bonds was 40% lower than that in the WF/PLA composites. Moreover, the increasing proportion of O–C=O bonds was much lower than the increase in C-O bonds. This difference was because BDICDI was not only a water scavenger but also an acid scavenger. For WF/PLA/1 wt% BDICDI composites, BDICDI absorbed the water penetrating into the WF/PLA/BDICDI composites and inhibited the hydrolysis of PLA. In addition, BDICDI reacted with the carboxylic acid formed by the hydrolysis of ester bonds, thereby inhibiting autocatalytic degradation and enhancing the stability of the WF/PLA composites. Therefore, BDICDI played a good stabilizing stabilization role and prolonged the service lives of WF/PLA/BDICDI composites.

GPC/LS data of three types of WF/PLA composites are shown in Table 5. With the addition of BDICDI, the molecular weight of PLA in the WF/PLA/BDICDI composites increased which indicated that BDICDI can be used as a chain extender for PLA [24]. As the soil burial time increased, the molecular weights of the three WF/PLA composite materials all decreased, which was caused by the hydrolysis of the ester bonds. The polydispersity index (PDI) did not change significantly as the degradation time increased. This finding indicated that in the early stage of soil degradation, the chain break of PLA was not random at the early stage of soil degradation [34]. The ester bonds located at both ends of the PLA molecular chains were broken into small molecules, and small-molecule carboxylic acid was formed. BDICDI is sensitive to small-molecule carboxylic acid, and thus BDICDI was more effective than PLA in reacting with the carboxylic acid formed by soil degradation, thereby inhibiting the autocatalytic effect of PLA [23, 26, 29]. It was consisted with our hypothesis that the BDICDI had stabilizing effect on the biodegradation of WF/PLA composites.

The stabilization mechanism of BDICDI on the WF/PLA composites is summarized in Fig. 4. As the soil burial time increased, the ester bonds on both sides of the PLA molecular chains were hydrolyzed and broken into small-molecules carboxylic acid. The BDICDI reacted with water permeating into the WF/PLA composites and the small-molecules carboxylic acid formed by the breaking of ester bonds. Acyl ureas and acid anhydrides were formed during the chemical reactions, and no longer affected the degradation of the WF/PLA composites [22, 24, 29]. BDICDI not only inhibited the hydrolysis of PLA chains, but also inhibited the autocatalytic degradation of PLA chains. Therefore, BDICDI could improve the stability of the WF/PLA/BDICDI composites.

Effects on the Surface Morphology

With increasing of soil burial time, the surface morphologies of the three WF/PLA composites exhibited different changes (Fig. 5). The color of the WF/PLA composites gradually became lighter, and an increasing number of white spots appeared on the surfaces of the composites. After 150 days, the surfaces of the composites became opaque and almost completely whitened. This phenomenon can be explained by the infrared image (Fig. 1). The WF contained phenolic substances, and the phenolic substances darkened after being heated. Therefore, the color of the WF/PLA composites turned yellow after melting and blending. The peak at 798 cm^{-1} (Fig. 1) is the characteristic peak of the benzene ring in the phenolic substances in wood [35]. With increasing degradation time, this characteristic peak almost disappeared. The phenolic substances in the soil were dissolve as the soil burial time increased, which indicated that material exchanges occurred between the composites and the soil during the soil burial process. With the addition of WF, the ability of material exchanges between composites and external environment was enhanced. After 90 days of soil burial, black cracks gradually appeared on the surfaces of the WF/PLA composites

Table 5 GPC/LS data of three WF/PLA composites before and after soil burial

	Time (day)	Mn ($\times 10^4$ g/mol)	M_w ($\times 10^4$ g/mol)	PDI (Mw/Mn)
WF/PLA	0	5.227	6.642	1.27
	90	4.814	6.047	1.26
	150	3.658	4.731	1.29
WF/PLA 1 wt% BDICDI	0	6.888	7.797	1.13
	90	5.939	7.039	1.18
	150	5.923	6.820	1.15
WF/PLA 3 wt% BDICDI	0	6.767	7.784	1.15
	90	6.314	7.293	1.16
	150	5.958	7.006	1.17

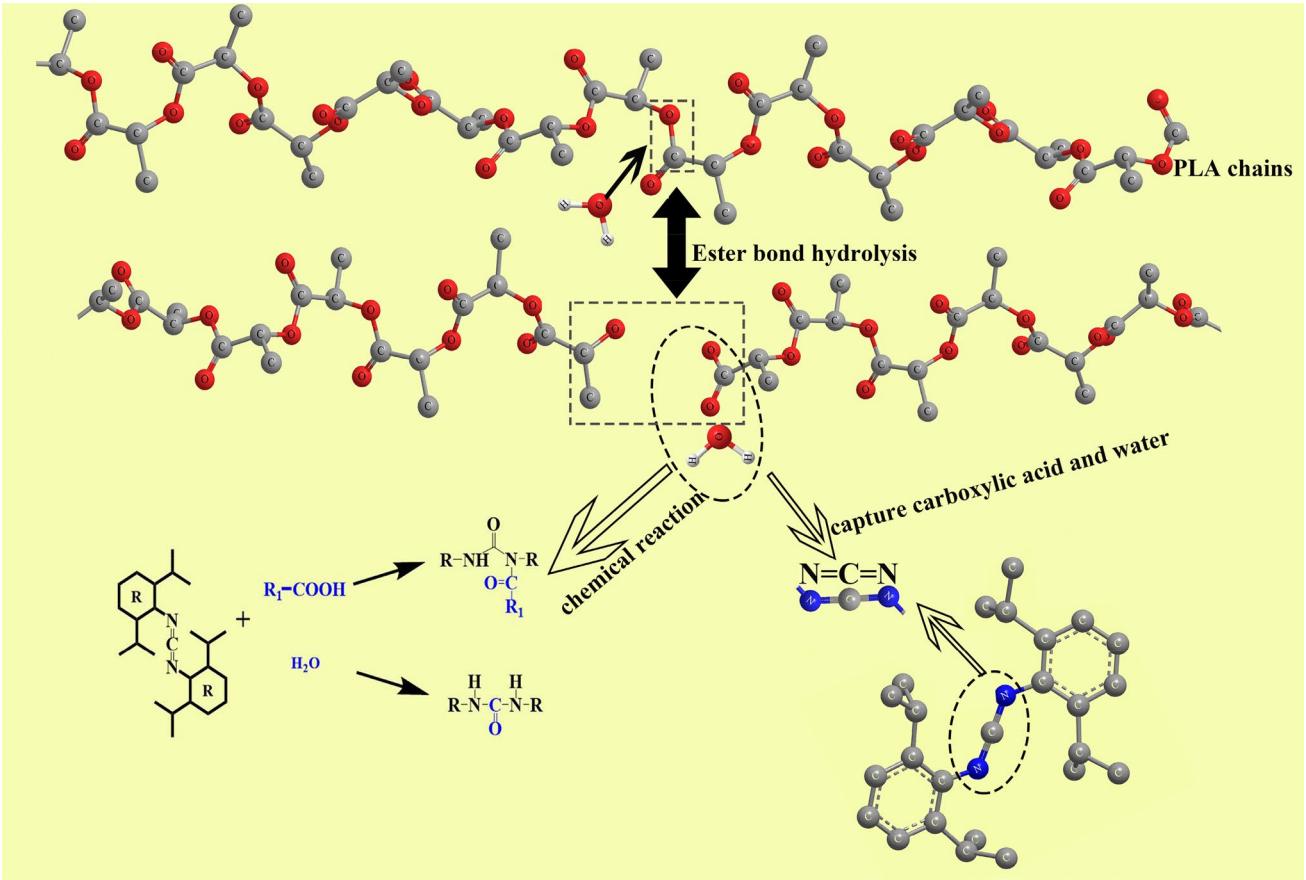

Fig. 4 Mechanism of BDICDI stabilized WF/PLA composites

without BDICDI. The cracks were caused by the stresses applied to the composites and the microbial invasion of the soil. In contrast, there were no cracks on the surfaces of the WF/PLA/1 wt% BDICDI or WF/PLA/3 wt% BDICDI composites. After 150 days of soil burial, many cracks appeared on the surfaces of the WF/PLA composites, whereas only slight cracks appeared on the surfaces of the composites containing BDICDI. This indicated that BDICDI could stabilize the surface morphologies of the WF/PLA/BDICDI composites, delay the cracks generated during its ultilization, and increased the service lives of the WF/PLA composites.

Evaluation of Composite Stability

From GPC/LS coupled system, the viscometry-average molecular weight (M_V) was determined by using GPC/LS coupled system and the Mark- Howink-Sakurada (MHS) equation was used to determine the intrinsic viscosity as follow:

$$[\eta] = KM_v^a \tag{2}$$

where [η] is intrinsic viscosity (mL/g), the K and 'a' parameters are given by the GPC/LS coupled system. In the MHS equation, the value of the 'a' parameter depends on the degree of branching of the polymer chains; moreover, the value of the 'a' parameter is negatively correlated with the degree of branching. Usually, the value of the 'a' parameter for linear PLA ranges from 0.77 to 0.64 [36]. The values of the 'a' parameter for the WF/PLA/1 wt% BDICDI and WF/PLA/3 wt% BDICDI composites were both below 0.64 (Fig. 6), which indicated that BDICDI linked the PLA molecular chains and that the degree of branching of the PLA molecular chains was increased. Moreover, the value of [η] can be used to obtain an approximate value of hydrodynamic radii (Rh) of PLA chains in the tetrahydrofuran solvent. The equation to evaluate 'Rh' and [η] is as follows:

$$\mathrm{Rh} = \left[\frac{(3 \times [\eta] \times \mathrm{M_w})}{10 \times \pi \times N_A}\right]^{1/3} \tag{3}$$

where, M_w is the average molecular weight and N_A (6.022×10^{23} mol^{-1}) is the Avogadro constant. Due to the effect of chain extension of BDICDI, the hydrodynamic radii of the WF/PLA/BDICDI composites increased compared to those of the WF/PLA composites (Fig. 6) [37]. The changes

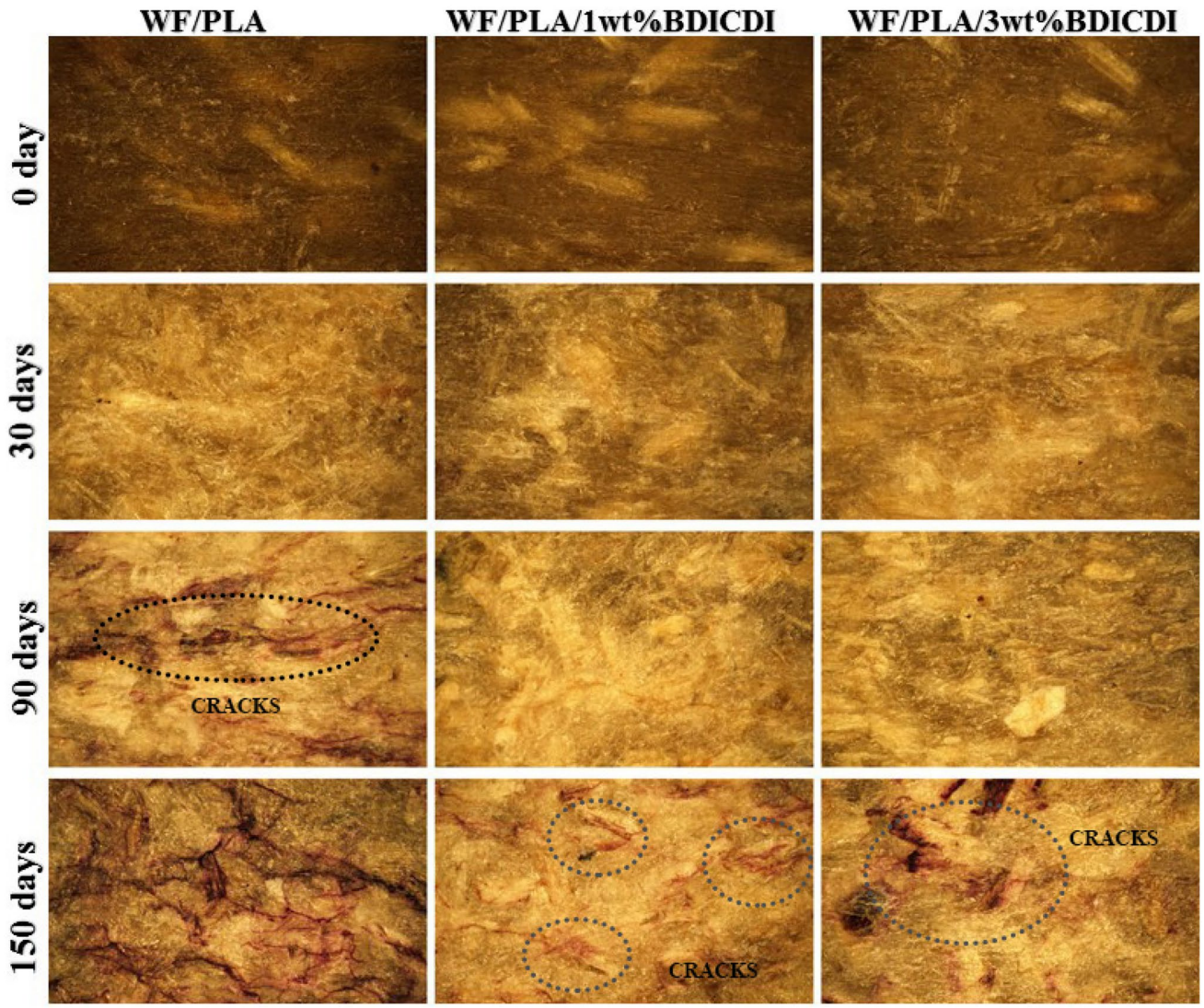

Fig. 5 Surface photos of composites before and after soil burial

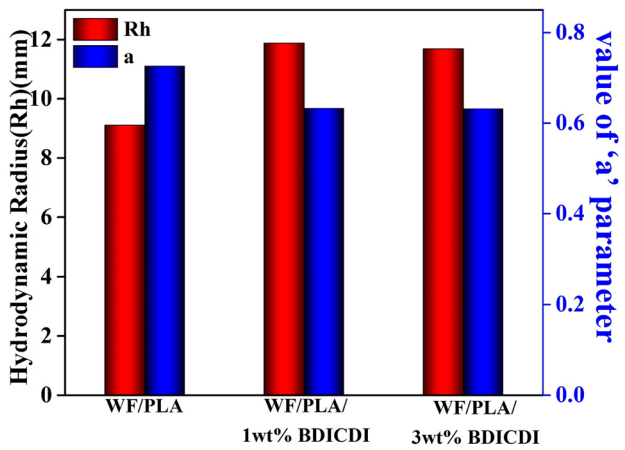

Fig. 6 Plots of the hydrodynamic radius and Mark-Houwink-Sakurada 'a' of composites

in Rh and the 'a' parameter confirmed that the reaction between BDICDI and PLA led to chain extension/branching.

Changes in the molecular chains of PLA inevitably led to changes in the crystallinity of the WF/PLA/BDICDI composites. The chemical effects of BDICDI of WF/PLA composites reached the limit at a BDICDI concentration of 1 wt%. Therefore, even with the addition of 3 wt% BDICDI, the molecular weight, Rh and 'a' values of PLA chains in the WF/PLA/BDICDI composites did not change significantly. The excess BDICDI further destroyed the crystallization (all DSC datas from the second heating), and thus the WF/PLA 3wt%BDICDI composites got the lowest crystallinity (Fig. 7d).

The crystallinity of the three WF/PLA composites increased gradually with the respect to the soil burial time (Fig. 7). The amorphous region of PLA was more sensitive

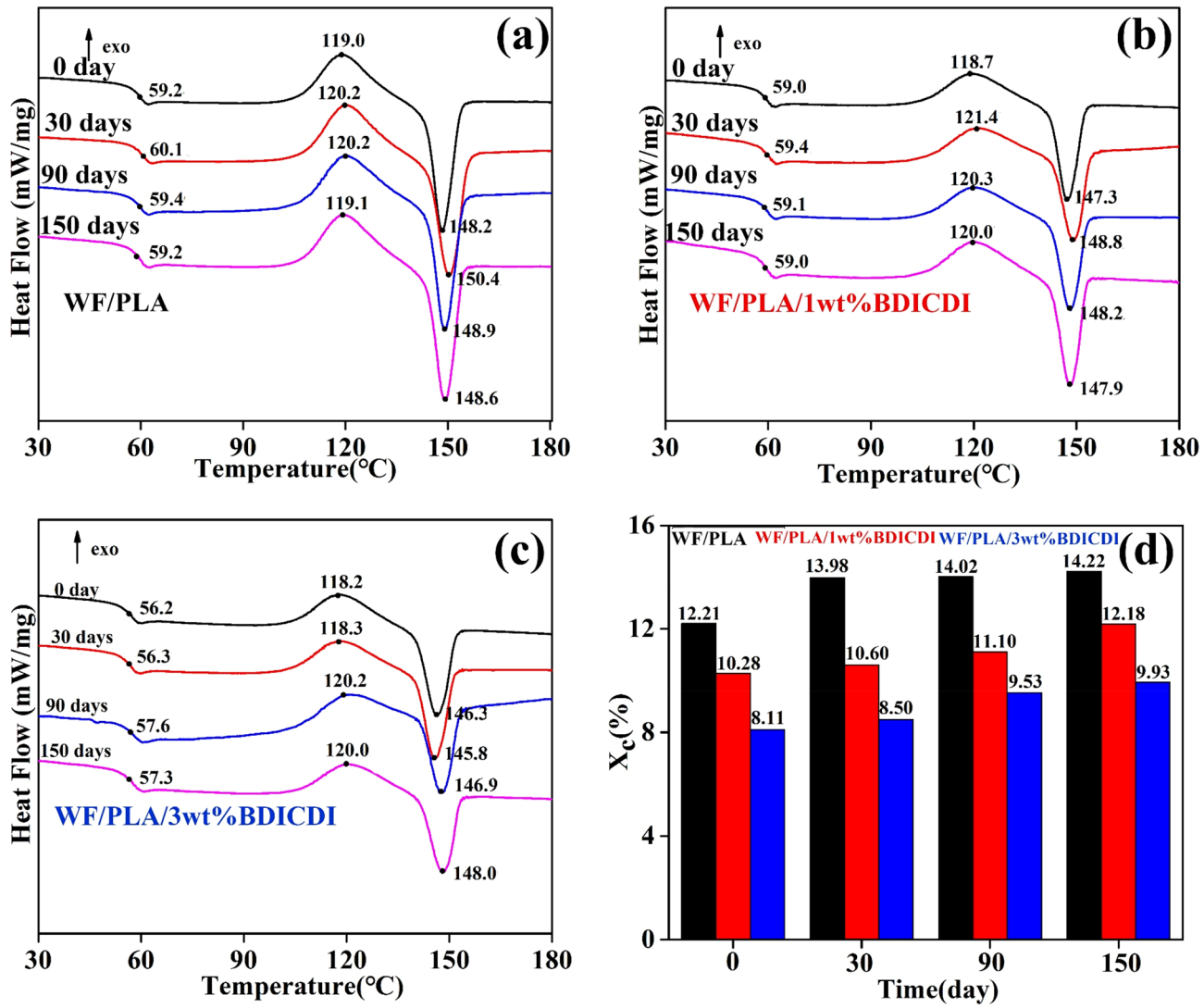

Fig. 7 DSC curves of **a** WF/PLA, **b** WF/PLA 1 wt% BDICDI, **c** WF/PLA 1 wt% BDICDI composites, **d** degree of crystallinity

to water than the crystallization region. This phenomenon can be interpreted as hydrolysis promoting the movement of molecular chains in the amorphous region which favors their crystallization [38]. Through comparison, the crystallinity of the WF/PLA/BDICDI composites increased slowly compare to the WF/PLA composites. After 30 days in the soil, the crystallinity of the WF/PLA composites increased by 14.5%, while that of WF/PLA/1 wt% BDICDI composites increased by only 7.9% even after 90 days of degradation. This further indicated that BDICDI stabilized the molecular chain of PLA, thereby ensuring the stability of the WF/PLA/BDICDI composites.

During the 150 days of soil burial, the glass transition temperatures (T_g) of the three composites remained basically stable. By the initial stage of the degradation of the three WF/PLA composites, the removal of the small molecular chains was not able to change the structure of the entire PLA molecular chains, which would not affect the value of the T_g. This was consistent with the conclusions from the previous chemical mechanism analysis, which showed that the degradation of PLA chains took place at the chain ends. After 30 days of soil burial, the melting (T_m) and cold crystallization temperatures (T_{cc}) of the composites increased, which was also reported in elsewhere [39]. It was suggested that the plasticization of water and smaller chains of PLA formed by degradation would increase the size of PLA crystallites, as well as its T_m and T_{cc}. With further degradation, the PLA crystal region was destroyed, which made the energy barrier to be overcome lower for PLA recrystallization. Therefore, the T_m and T_{cc} gradually decreased after 90 days of soil burial.

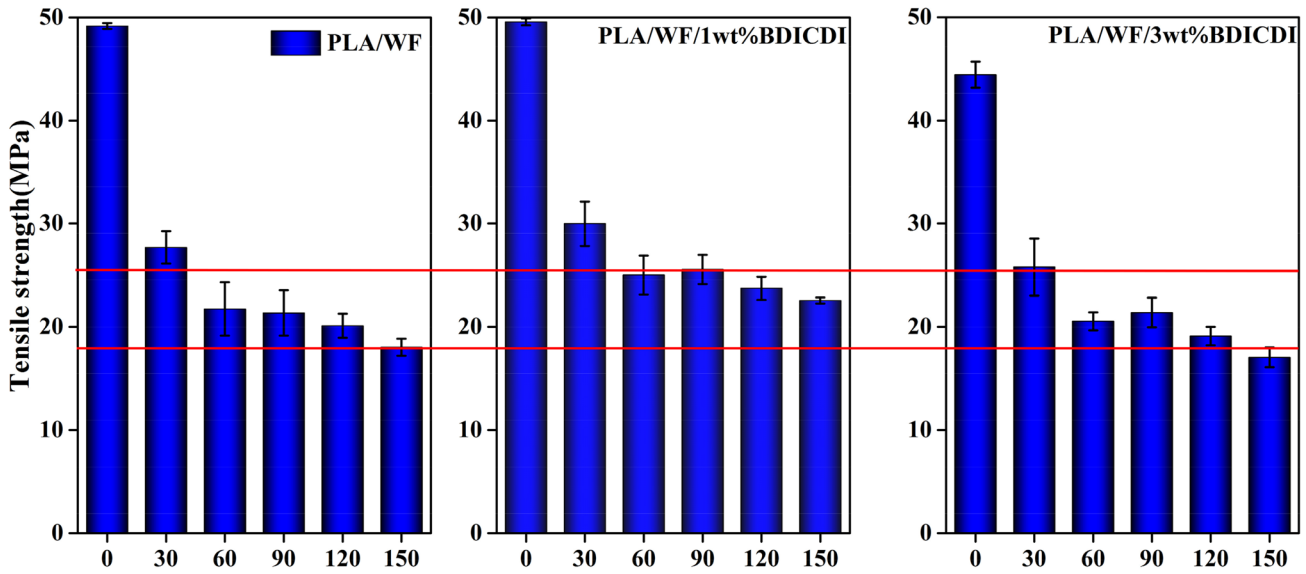

Fig. 8 Tensile strength evolution of WF/PLA composites

Tensile Strength Changes

Scince WF/PLA composites are used to replace disposable plastics with short service lives, it is important for the composites to maintain mechanical stability during use. Changes in the tensile strengths of the three WF/PLA composites under a real-use environment are shown in Fig. 8. After the addition of 1 wt% BDICDI, the tensile strengths of the WF/PLA/1 wt% BDICDI composites increased slightly. This increase in strength was because BDICDI created a strong interaction between WFs and BDICDI, which promoted better interfacial adhesion between PLA and WFs [29]. However, thw effect of BDICDI was limited. When 3 wt% of BDICDI was added to the composites, the excess BDICDI destroyed the interface between PLA and WF, which decreased the tensile strength.

After 150 days of soil burial, the tensile strengths of the composites decreased in different trends. The tensile strengths of the unmodified WF/PLA composites decreased while those of WF/PLA/1 wt% BDICDI remained stable from 30 to 120 days. After 120 days of soil burial, the tensile strengths of the WF/PLA/1 wt% BDICDI composites was 1.31 times to those of the WF/PLA composites. This showed that adding 1 wt% BDICDI effectively stabilized the WF/PLA composites. Although the composites containing 3 wt% of BDICDI exhibited some stability, the tensile strengths of these composites also decreased rapidly due to the structual damage caused by the excessive BDICDI.

Conclusions

BDICDI can be used as a chain extender of PLA. The extension of chains increased the branching of the PLA chains. From the mechanism of maintaining the stability of the WF/PLA composites, BDICDI was a good water removal agent and acid scavenger. BDICDI captured water that penetrated into the composites. Additionally, BDICDI captured carboxylic acid formed by the hydrolysis of ester bonds to inhibit the autocatalytic degradation of PLA. The addition of BDICDI effectively maintained the stability of the WF/PLA composites during soil burial. The addition of 1 wt% BDICDI had the best tensile strength and stabilization effect on the WF/PLA composites. After 120 days of soil burial, the tensile strengths of WF/PLA/1 wt% BDICDI composites were 1.31 times to those of the WF/PLA composites. This study provides a basis for WF/PLA/1 wt% BDICDI composites to replace single-use plastics as packaging or agricultural materials. And it broadens the application of WF/PLA/1 wt% BDICDI composites.

Acknowledgements This work was supported by the Fundamental Research Funds for the Central Universities (No. 2572017EB06) and the National Natural Science Foundation of China (No. 31670569). Special thanks were to the support of the Chinese University Students 'Innovation and Entrepreneurship Project (CL201910).

References

1. Rochman CM et al (2013) Classify plastic waste as hazardous. Nature 494(7436):169–171

2. Liu M et al (2018) Microplastic and mesoplastic pollution in farmland soils in suburbs of Shanghai, China. Environ Pollut 242:855–862
3. Schnurr REJ et al (2018) Reducing marine pollution from single-use plastics (SUPs): a review. Mar Pollut Bull 137:157–171
4. Auta HS et al (2017) Distribution and importance of microplastics in the marine environment: a review of the sources, fate, effects, and potential solutions. Environ Int 102:165–176
5. Provencher JF et al (2017) Quantifying ingested debris in marine megafauna: a review and recommendations for standardization. Anal Methods-UK 9(9):1454–1469
6. Wilcox C et al (2016) Threat of plastic pollution to seabirds is global, pervasive, and increasing. Proc Natl Acad Sci USA 113(4):E491
7. Provencher JF et al (2018) Garbage in guano? Microplastic debris found in faecal precursors of seabirds known to ingest plastics. Sci Total Environ 644:1477–1484
8. Anbumani S et al (2018) Ecotoxicological effects of microplastics on biota: a review. Environ Sci Pollut R 25(15):14373–14396
9. Lei L et al (2018) Microplastic particles cause intestinal damage and other adverse effects in zebrafish *Danio rerio* and nematode *Caenorhabditis elegans*. Sci Total Environ 619:1–8
10. Song G et al (2018) Packaging waste from food delivery in China's mega cities. Resour Conserv Recycl 130:226–227
11. Price AJ et al (2018) Effects of integrated polyethylene and cover crop mulch, conservation tillage, and herbicide application on weed control, yield, and economic returns in watermelon. Weed Technol 32(5):623–632
12. Voznyak Y et al (2018) Ductility of polylactide composites reinforced with poly (butylene succinate) nanofibers. Compos Part A-Appl S 90:218–224
13. Yatigala et al (2018) Compatibilization improves physico-mechanical properties of biodegradable biobased polymer composites. Compos Part A-Appl S 107:315–325
14. Awal A et al (2015) Thermorheological and mechanical properties of cellulose reinforced PLA bio-composites. Mech Mater 80:87–95
15. Zhao S et al (2018) Fully bio-based soybean adhesive in situ cross-linked by interactive network skeleton from plant oil-anchored fiber. Ind Crop Prod 122:366–374
16. Gorrasi G et al (2013) Effect of PLA grades and morphologies on hydrolytic degradation at composting temperature: Assessment of structural modification and kinetic parameters. Polym Degrad Stabil 98(5):1006–1014
17. Stloukal P et al (2015) Kinetics and mechanism of the biodegradation of PLA/clay nanocomposites during thermophilic phase of composting process. Waste Manage 42:31–40
18. Kaynak C et al (2016) Accelerated weathering performance of polylactide and its montmorillonite nanocomposite. Appl Clay Sci 121:86–94
19. Lv S et al (2018) Enhanced durability of sustainable poly(lactic acid)-based composites with renewable starch and wood flour. J Clean Prod 203:328–339
20. Petinakis E et al (2010) Biodegradation and thermal decomposition of poly(lactic acid)-based materials reinforced by hydrophilic fillers. Polym Degrad Stabil 95(9):1704–1707
21. Lv S et al (2016) Modification of wood flour/PLA composites by reactive extrusion with maleic anhydride. J Appl Polym Sci 133:4329515
22. Chen F et al (2008) Performance enhancement of poly(lactic acid) and sugar beet pulp composites by improving interfacial adhesion and penetration. Ind Eng Chem Res 47(22):8667–8675
23. Stloukal P et al (2016) (2016) Carbodiimide additive to control hydrolytic stability and biodegradability of PLA. Polym Test 54:19–28
24. Zhao Y, Ding S, Yuan Y, Wang Y (2014) Enhanced degradation stability of poly (p-dioxanone) under different temperature and humidity with bis-(2,6-diisopropylphenyl) Carbodiimide. J Appl Polym Sci 131:400266
25. Chen A, Wei K, Jeng R, Lin J, Dai SA (2011) Well-defined polyamide synthesis from diisocyanates and diacids involving hindered carbodiimide intermediates. Macromolecules 44(1):46–59
26. Yang L, Chen X, Jing X (2008) Stabilization of poly(lactic acid) by polycarbodiimide. Polym Degrad Stabil 93(10):1923–1929
27. Kucharczyk P, Hnatkova E, Dvorak Z, Sedlarik V (2013) Novel aspects of the degradation process of PLA based bulky samples under conditions of high partial pressure of water vapour. Polym Degrad Stabil 98(1):150–157
28. Martucci JF, Ruseckaite RA (2015) Biodegradation behavior of three-layer sheets based on gelatin and poly(lactic acid) buried under indoor soil conditions. Polym Degrad Stabil 116:36–44
29. Holcapkova P, Stloukal P, Kucharczyk P, Omastova M, Kovalcik A (2017) Anti-hydrolysis effect of aromatic carbodiimide in poly(lactic acid)/wood flour composites. Composites A 103:283–291
30. Lipsa R, Tudorachi N, Darie-Nita RN, Oprica L, Vasile C, Chiriac A (2016) Biodegradation of poly(lactic acid) and some of its based systems with *Trichoderma viride*. Int J Biol Macromol 88:515–526
31. Spiridon I, Paduraru OM, Zaltariov MF, Darie RN (2013) Influence of keratin on polylactic acid/chitosan composite properties, behavior upon accelerated weathering. Ind Eng Chem Res 52(29):9822–9833
32. Cairns M, Sykes A, Dickson GR, Orr JF, Farrar D, Dumba A (2011) Through-thickness control of polymer bioresorption via electron beam irradiation. Acta Biomater 7(2):548–557
33. Mansouri M, Berrayah A, Beyens C, Rosenauer C, Jama C, Maschke U (2016) Effects of electron beam irradiation on thermal and mechanical properties of poly(lactic acid) films. Polym Degrad Stabil 133:293–302
34. Sednickova M, Pekarova S, Kucharczyk P, Bockaj J, Janigova I, Kleinova A (2018) Changes of physical properties of PLA-based blends during early stage of biodegradation in compost. Int J Biol Macromol 113:434–442
35. Hamedan HJ, Sohani MM, Aalami A, Nazarideljou MJ (2019) Genetic engineering of lignin biosynthesis pathway improved stem bending disorder in cut gerbera (*Gerbera jamesonii*) flowers. Sci Hortic-Amst 245:274–279
36. Najafi N, Heuzey MC, Carreau PJ, Wood-Adams PM (2012) Control of thermal degradation of polylactide (PLA)-clay nanocomposites using chain extenders. Polym Degrad Stabil 97(4):554–565
37. Al-Itry R, Lamnawar K, Maazouz A (2014) Reactive extrusion of PLA, PBAT with a multi-functional epoxide: physico-chemical and rheological properties. Eur Polym J 58:90–102
38. Rocca-Smith JR et al (2017) Effect of the state of water and relative humidity on ageing of PLA films. Food Chem 236:109–119
39. Tsuji H et al (2015) Properties and morphology of poly(L-lactide) III Effects of initial crystallinity on long-term in vitro hydrolysis of high molecular weight poly(L-lactide) film in phosphate-buffered solution. J Appl Polym Sci 77(7):1452–1464